



Supplement of

Implementation of HONO into the chemistry–climate model CHASER (V4.0): roles in tropospheric chemistry

Phuc Thi Minh Ha et al.

Correspondence to: Phuc Thi Minh Ha (hathiminh.phuc@gmail.com)

The copyright of individual parts of the supplement might differ from the article licence.

Supplements

Table S 1: Lists of EANET stations grouped by their countries with ID numbers in parenthesis.

Country	Station (ID number)
Cambodia	PhnomPenh (31)
China	Jinyunshan (48), Hongwen (14)
Indonesia	Jakarta (18), Serpong (36), Bandung (1)
Japan	Rishiri (33), Ochiishi (26), Tappi (38), Sado-seki (34), Happo (10), Ijira (15), Oki (28), Banryu (3), Yusu-hara (45), Hedo (11), Ogasawara (27), Tokyo (40)
Lao	Vientiane (42)
Malaysia	Petaling Jaya (30), Tanah Rata (37), Danum Valley (7)
Mongolia	Ulaanbaatar (41), Terelj (39)
Myanmar	Yangon (43), Mandalay (50)
Philippines	Metro Manila (22), Mt. Sto. Tomas (24)
Republic of Korea	Kanghwa (19), Cheju (Kosan) (5), Imsil (16)
Russia	Mondy (23), Listvyanka (21), Irkutsk (17), Primorskaya (32)
Thailand	Bangkok (2), Samutprakarn (47), Pathumthani (29), Khanchanaburi (20), Chiang Mai (6), Sakaerat (35), Nai Mueang (25), Chang Phueak (46), Si Phum (49)
Vietnam	Hanoi (8), Hanoi (Relocated) (9), Hoa Binh (13), Can Tho (4), Ho Chi Minh (12), Yen Bai (44)

5 Table S 2: Model comparison with ATom1 flights, calculated for all flights and North Pacific (NP) region: no outlier detection is applied. N is the available data for each calculation, and R is the correlation coefficient. R and bias of the STD run are shown as bold if better than that of the OLD run. Unit of bias is ppt for NO₂, OH, ppb for O₃, CO.

	NO ₂	NO ₂ (NP)	O ₃	O ₃ (NP)	OH	OH (NP)	CO	CO (NP)
N	29,509	2,283	29,204	2,246	7,601	608	27,467	2,172
R (STD)	0.730	0.621	0.751	0.609	0.579	0.407	0.659	0.596
R (OLD)	0.697	0.306	0.752	0.598	0.584	0.374	0.643	0.596
bias (STD)	-11.277	0.588	11.637	8.471	-0.038	-0.003	1.698	-1.713
bias (OLD)	-6.940	4.450	15.025	13.050	-0.015	0.015	-7.521	-12.393

10 **Table S 3: Additional sensitivity runs for the EMeRGe comparison.**

The AIRC case aims to evaluate the source of HONO from aircraft emissions of HONO using a HONO/NO_x emission factor of 0.4. In the EMx8 case, the HONO/NO_x emission factor is amplified up to 0.8 (=0.1 in STD case) to emphasize the sensitivity of HONO's direct source from the ground layer, especially from soils (Oswald et al., 2013). In the GRx8 case, the rate constant of (R2) is eightfold to increase homogeneous HONO production, given that daytime missing HONO could relate to other gas-phase formations (Romer et al., 2018; Li et al., 2014). In the EMx8 and GRx8 cases, factor 8 is selected after testing with 2 and 4, aiming for simulations to agree with the measurements.

No.	Simulation ID	Description	Note
1	AIRC	aircraft HONO emission = 0.4% aircraft NO _x emission	Not applied in STD
2	GRx8	Rate (R2) × 8	
3	EMx8	EM(HONO) = 0.8 NO _x emission	= 0.1 in STD

15

Table S 4: Tables of correlation coefficient (*R*) and model biases against EMeRGe measurements for HONO.

“Alt.” columns show altitude ranges (±500 m). The “*N*” column shows the numbers of hourly-averaged values calculated for each altitude range. Left table: darker colours represent higher absolute *R* values (closer to ±1). Right table: lighter colours show smaller model biases (closer to 0). The darkness of blues (negative values) and reds (positive values) are scaled to ±1 for *R* and ±maximum values of each row for biases. Unit of biases is ppt for HONO and NO₂, ppb for O₃ and CO.

Alt. <i>N</i>		<i>R</i> (HONO)											Bias(HONO)											20			
		STD	GRx8	EMx8	AIRC	maxST	ratR4	ratR4	+CLD	JANO3-B	JANO3-C	maxST+	JANO3-B	maxST+	JANO3-C	NEW	GRx8	EMx8	AIRC	maxST	ratR4	ratR4	+CLD	JANO3-B	JANO3-C	maxST+	JANO3-B
0	970	-0.23	-0.39	-0.29	-0.27	-0.17	-0.22	-0.21	0.63	0.62	0.64	0.63	-112.5	-94.1	-102.7	-112.2	-70.3	-106.1	-102.9	-21.7	-17.6	155.0	154.9				
1000	1714	0.49	0.36	0.51	0.44	0.56	0.24	0.24	0.36	0.37	0.48	0.48	-105.3	-95.5	-94.2	-105.6	-71.7	-99.8	-96.1	-47.8	-40.8	65.9	72.3				
2000	1538	0.31	0.47	0.38	0.36	0.47	0.12	0.07	0.47	0.40	0.41	0.39	-64.1	-62.9	-64.1	-64.4	-61.8	-63.3	-62.8	-53.1	-45.6	-32.5	-23.6				
3000	2296	0.16	0.05	0.11	0.11	-0.03	0.13	0.05	0.34	0.28	0.18	0.26	-44.2	-42.8	-44.1	-44.2	-43.2	-43.9	-43.7	-38.7	-30.2	-27.7	-16.2				
4000	192	-0.17	-0.24	-0.08	-0.11	0.28	-0.11	-0.04	0.08	-0.14	0.36	0.30	-26.0	-24.3	-25.8	-26.0	-25.6	-25.7	-25.4	-23.8	-17.9	-21.2	-14.4				
5000	836	0.04	0.03	0.14	0.21	0.53	0.19	0.75	0.17	-0.22	0.49	0.06	-18.9	-17.3	-18.8	-19.0	-18.5	-18.8	-18.3	-17.7	-12.8	-15.6	-9.6				
6000	506	-0.01	0.02	-0.03	0.03	0.11	-0.03	0.05	0.10	-0.26	0.16	-0.12	-5.0	-2.9	-4.6	-5.1	-4.9	-4.8	-4.8	-4.1	2.5	-3.9	2.2				
7000	76	-0.31	-0.33	-0.31	-0.33	-0.30	-0.30	-0.30	-0.29	-0.29	-0.27	-0.22	-4.1	0.7	-3.5	-4.3	-4.1	-3.8	-3.7	-2.3	1.5	-2.0	1.7				
8000	44	-0.67	-0.64	-0.64	-0.64	-0.64	-0.68	-0.67	-0.62	-0.65	-0.63	-0.59	-2.8	2.9	-1.9	-2.7	-2.7	-2.5	-2.5	-1.5	2.9	-1.2	3.5				

Table S 5: CH₄ lifetime and tropospheric abundances for NO_x, O₃, CO, and HONO and their changes by HONO chemistry in sensitivity cases.

Simulation ID	CH ₄ lifetime (yr)	Abundances of tropospheric			
		NO _x	O ₃	CO	HONO
		(TgN)	(TgO ₃)	(TgCO)	(TgN)
OLD	9.09	0.119	408.79	327.20	
STD	10.28	0.094	388.21	354.57	1.40
maxST	14.54	0.048	323.80	425.31	7.79
ratR4+CLD	9.60	0.108	390.34	337.68	3.18
JANO3-A	10.05	0.096	391.11	349.91	1.45
JANO3-B	7.60	0.116	426.89	292.29	2.02
JANO3-C	5.39	0.153	477.48	237.59	2.93
maxST+JANO3-B	10.20	0.057	351.27	357.27	12.64
maxST+JANO3-C	6.44	0.084	408.69	268.74	17.13
Effects	Changes (%)				
	vs OLD				vs STD
By STD	+13.05	-20.40	-5.03	+8.36	
by maxST	+50.65	-55.44	-17.84	+37.02	+634.51
by ratR4+CLD	+5.60	-8.57	-4.51	+3.20	+129.94
By JANO3-A	+10.57	-18.97	-4.32	+6.94	+3.42
By JANO3-B	-16.39	-2.49	+4.43	-11.06	+44.2
By JANO3-C	-40.74	+28.89	+16.08	-32.41	+108.7
By maxST+JANO3-B	+12.21	-52.10	-14.07	+9.19	+802.86
By maxST+JANO3-C	-29.15	-29.41	-0.02	-17.87	+1123.57

35

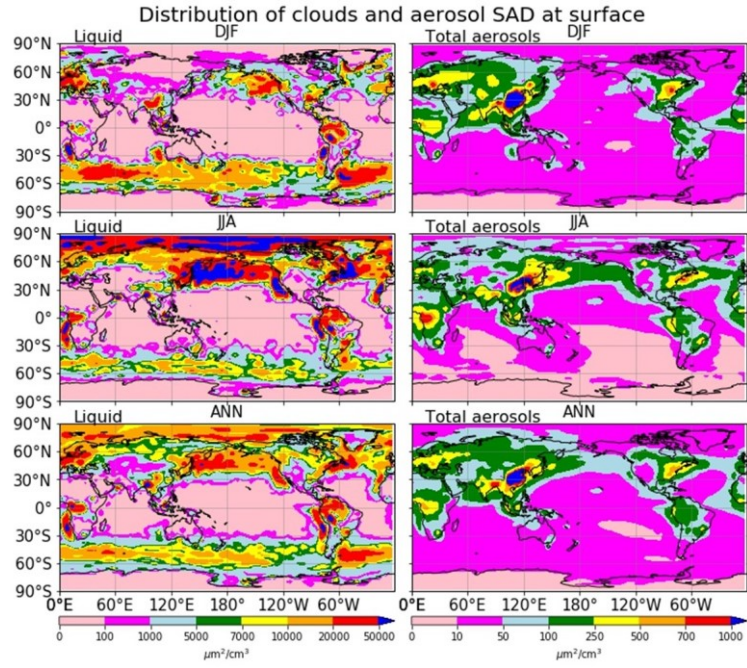


Figure S 1: Seasonal and annual mean distributions of SAD for clouds (left) and total aerosols (right)

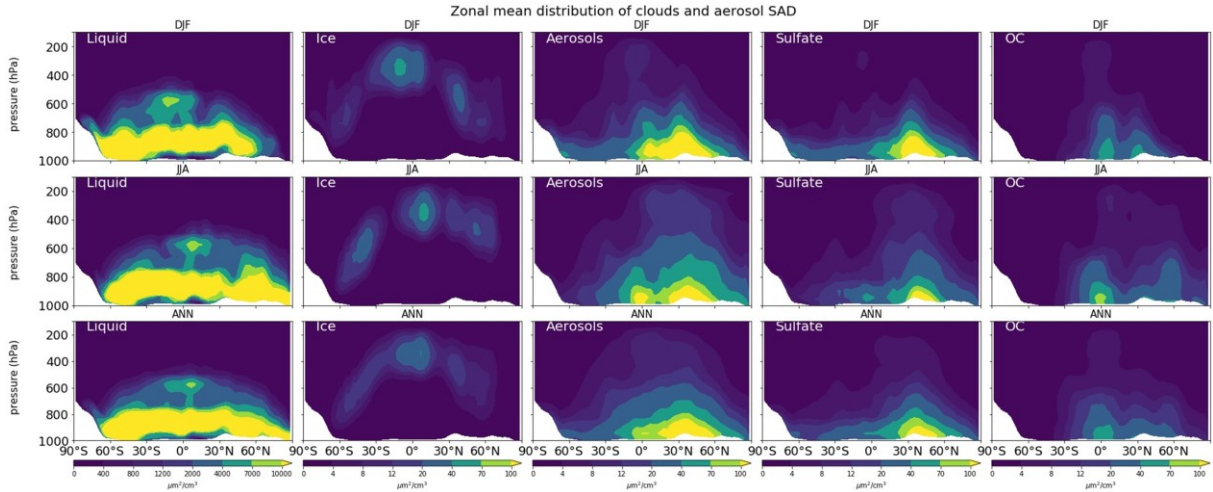


Figure S 2: Zonal, seasonal mean (upper and middle panels), and annual mean (lower panels) distribution of surface area density (SAD) for liquid clouds, ice cloud, total aerosol, sulfate aerosol, and organic carbon (from left to right).

40

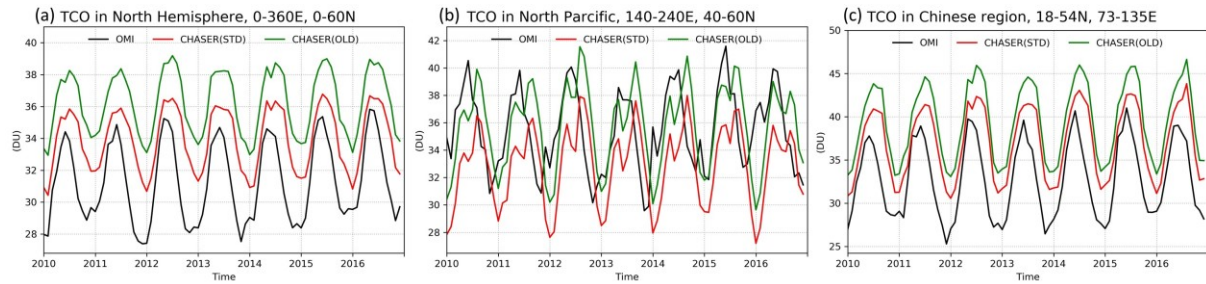
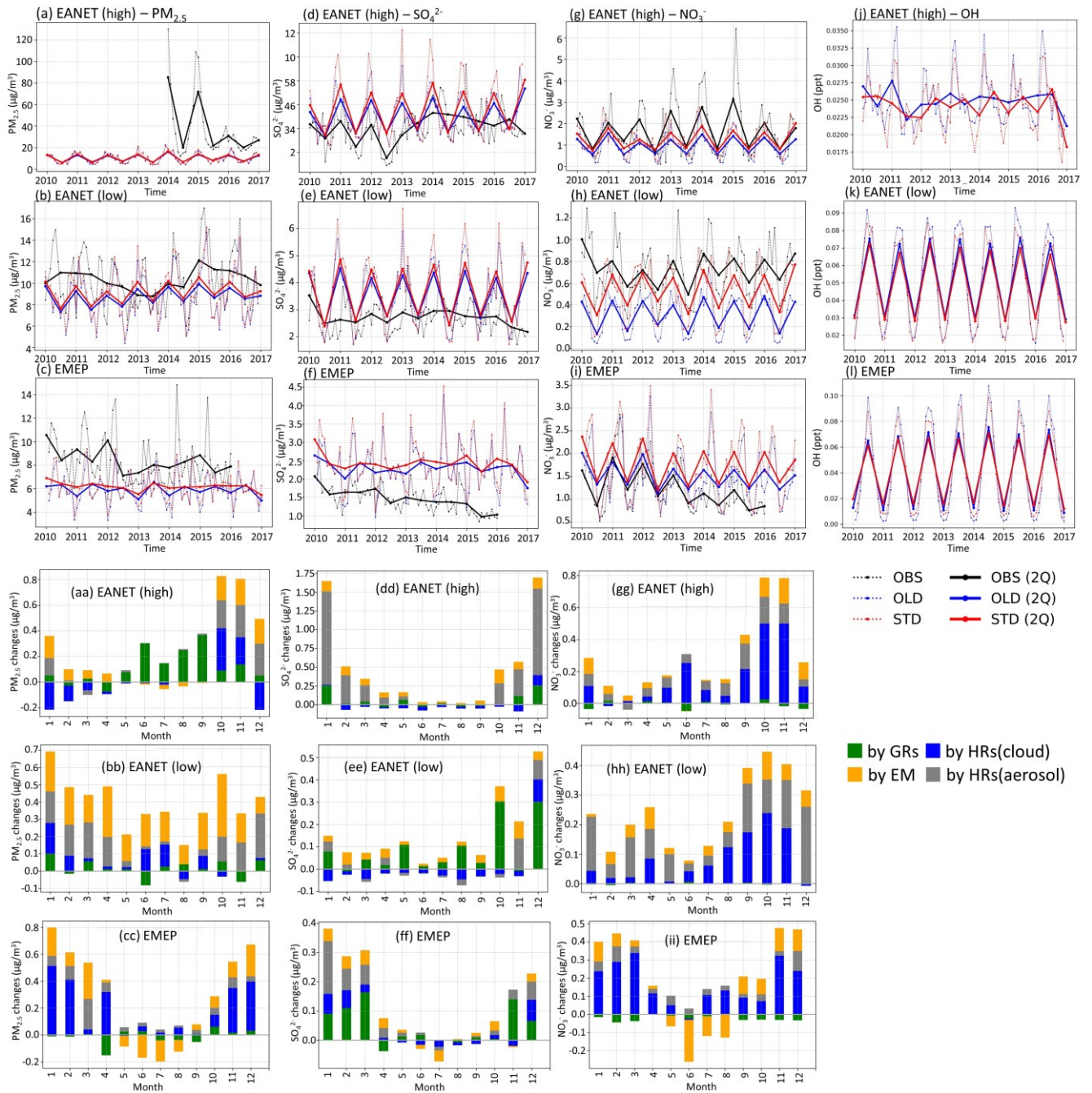


Figure S 3: Verifications with OMI satellite data for tropospheric column ozone (TCO). TCO (DU) by OMI (black) and CHASER (red: STD case; green: OLD case) in the Northern Hemisphere (a), NP (b), and Chinese (c) regions are plotted.



45 **Figure S 4: Grouped by observed and simulated mass concentrations (a-l) and monthly-mean changes (aa-ii) for $PM_{2.5}$, SO_4^{2-} , NO_3^-**
, and OH for EANET and EMEP stations, grouped as high- NO_x EANET, low- NO_x EANET, and all EMEP stations. In (a-m), black
lines: observation; red: STD case; blue: OLD case. Dotted lines are all stations' median from monthly-mean for each station in that
group. Thick solid lines represent two quarters averaged from dotted lines. There are no observational data for OH's plots (j-l), and
only values from STD and OLD simulations are presented. In (aa-ii), green bars: monthly changes by GRs; blue: by HRs on clouds;
50 **grey: by HRs on aerosols; orange: by EM.**

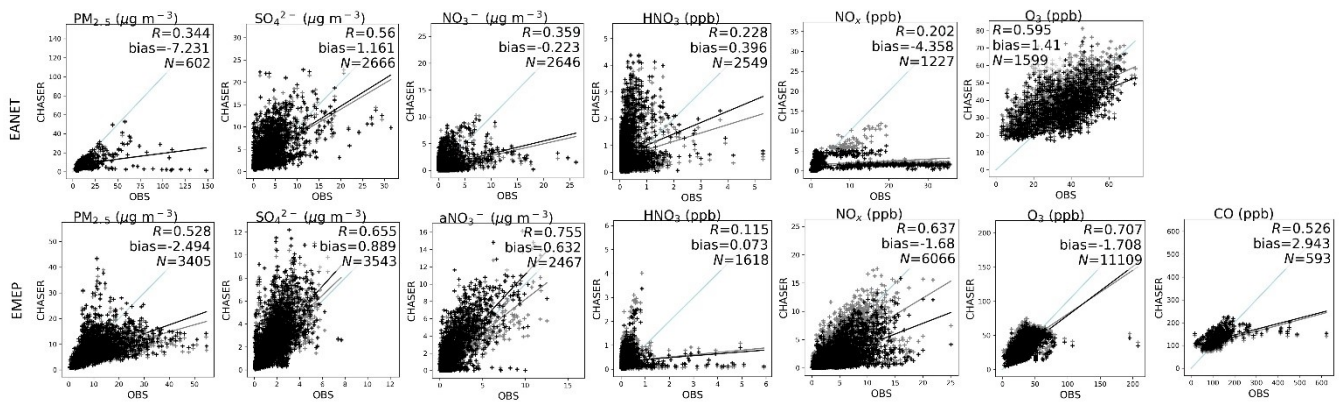


Figure S 5: Correlations of STD and OLD runs with EANET (upper) and EMEP (lower) stations for $PM_{2.5}$, SO_4^{2-} , NO_3^- , HNO_3 , NO_x , O_3 , and CO (CO for EMEP only). Fitting lines for STD (black) and OLD (grey) with observations are also plotted. N (no unit) is the number of available data after outlier filtering.

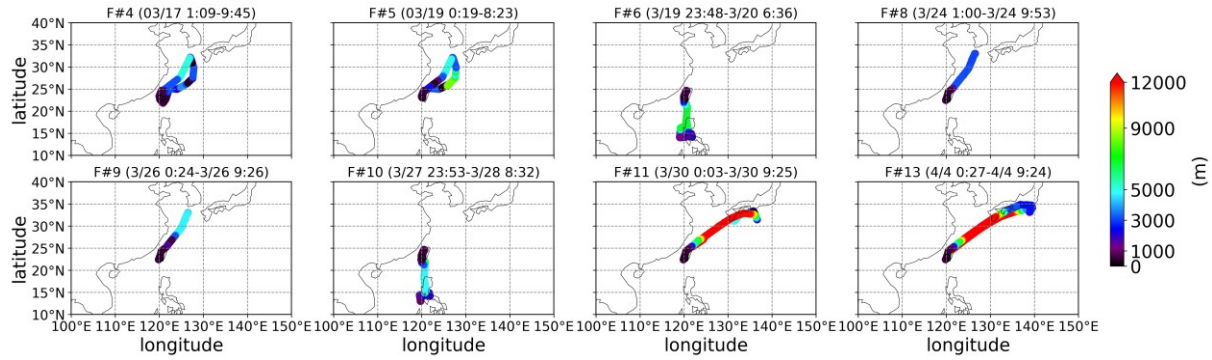


Figure S 6: Crushing altitudes in EMERGE-Asia 2018 campaign.

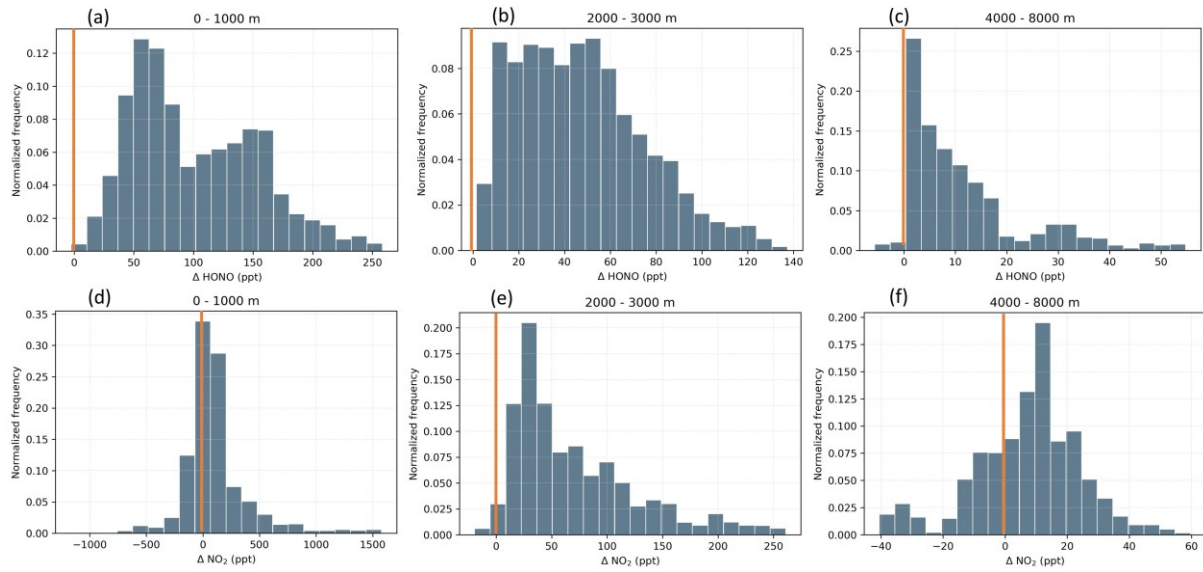


Figure S 7: Normalized distributions of the differences between measured and simulated data (OBS - STD) for HONO (upper panel) and NO_2 (lower panel). Data are separated into three categories (± 500 m): 0 - 1000 m (a-d), 2000 - 3000 m (b-e), 4000 - 8000 m (c-f). Three-sigma-rule outlier detection is applied for each altitude range before grouping.

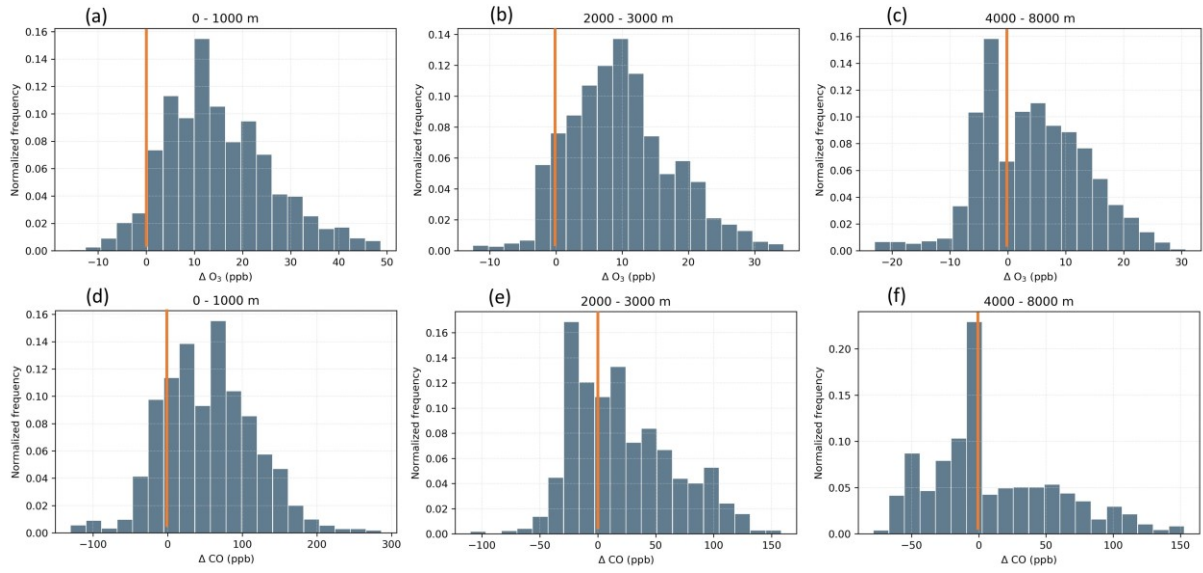


Figure S 8: Normalized distributions of the differences between measured and simulated data (OBS – STD) for O₃ (upper panels) and CO (lower panels). Data are separated into three categories (± 500 m): 0 – 1000 m (a-d), 2000 – 3000 m (b-e), 4000 – 8000 m (c-f). Outliers of each altitude group are filtered by a 3-order rule.

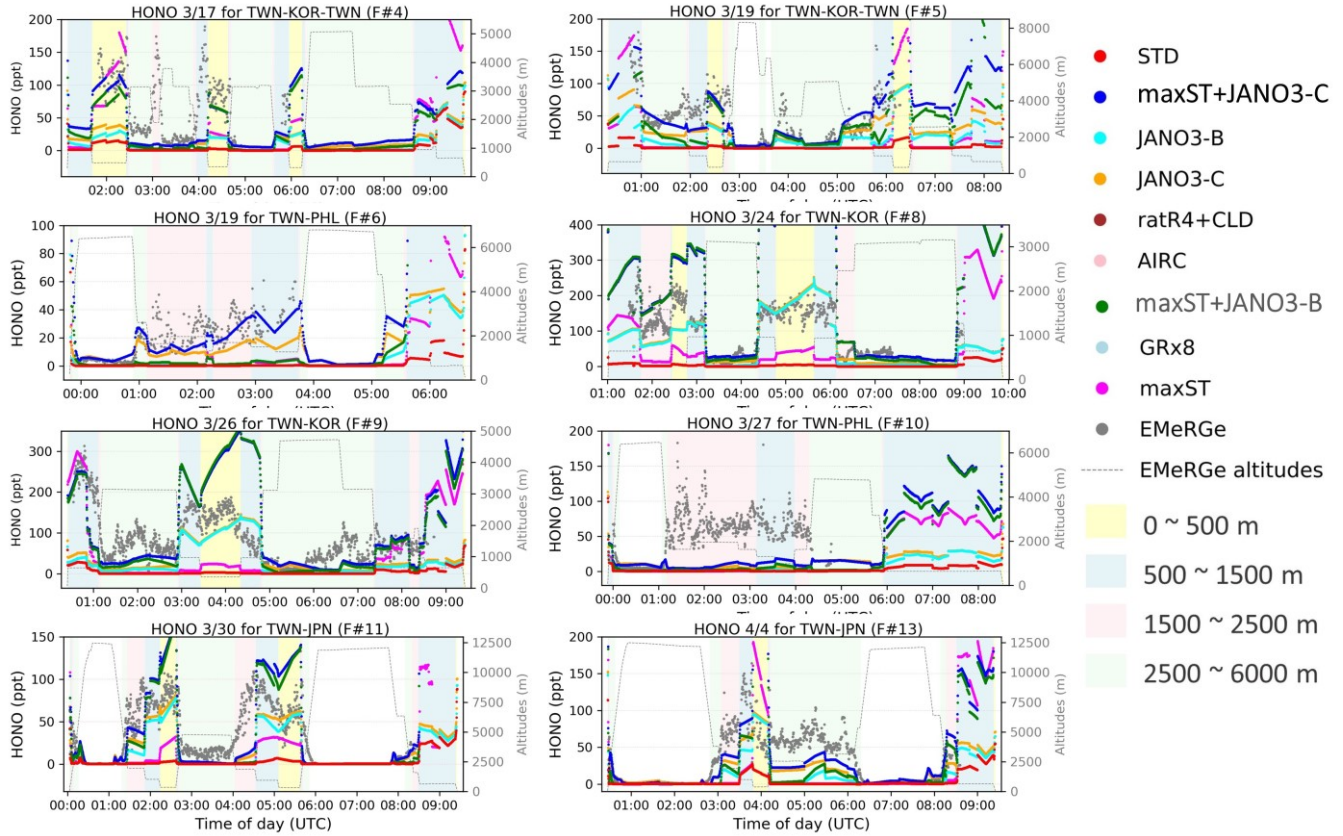


Figure S 9: HONO concentrations measured in EMeRGe flights. The observational values (grey dots), the STD case (red), the maxST case (magenta), maxST+JANO3-B case (green lines), and maxST+JANO3-C cases (blue lines) are plotted. Flight altitudes (metres) are plotted in light dash lines scaled to the right axis. Vertical background columns indicate altitude ranges.

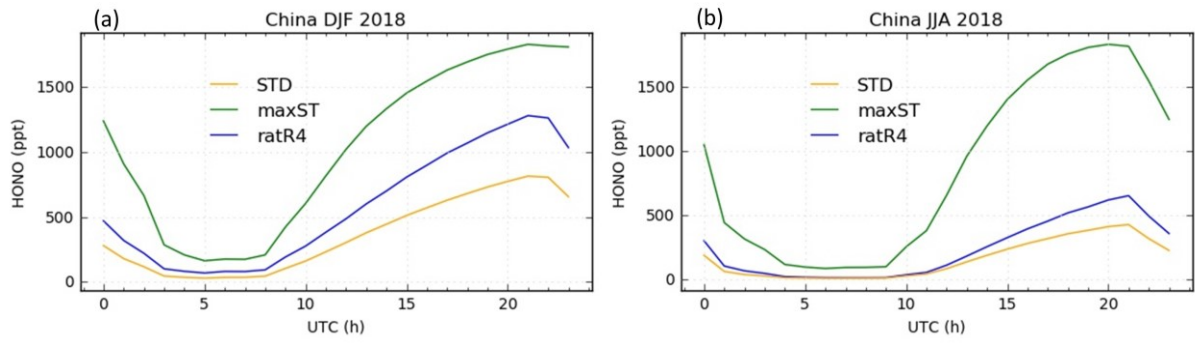


Figure S 10: Diurnal variance of HONO at the surface of the Chinese region in December, January, February (a), and June, July, August (b). Orange lines show STD run; green lines show maxST run; blue lines show ratR4 run. In (b), the averaged summer mean of HONO in surface air reached the maximum at 0.8 ppb in the STD simulation (orange), which substantially increased up to 1.8 ppb in maxST (green), which is closer to 2.0 ppb, as reported by Li et al. (2012).

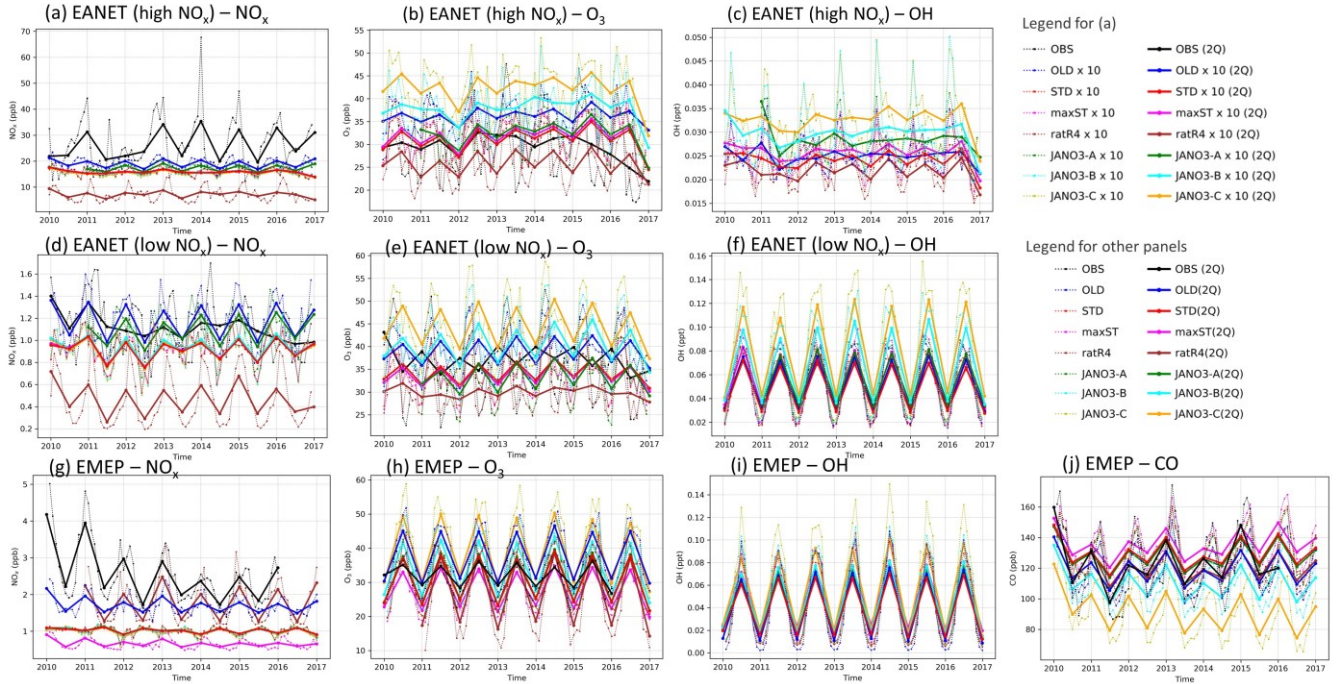


Figure S 11: Concentrations of NO_x, O₃, OH, and CO for EANET and EMEP stations by observation and various simulations. The upper legend block indicating simulated NO_x concentrations is tenfold for high-NO_x EANET stations (a panel). The lower legend block is for the other panels of the figure.

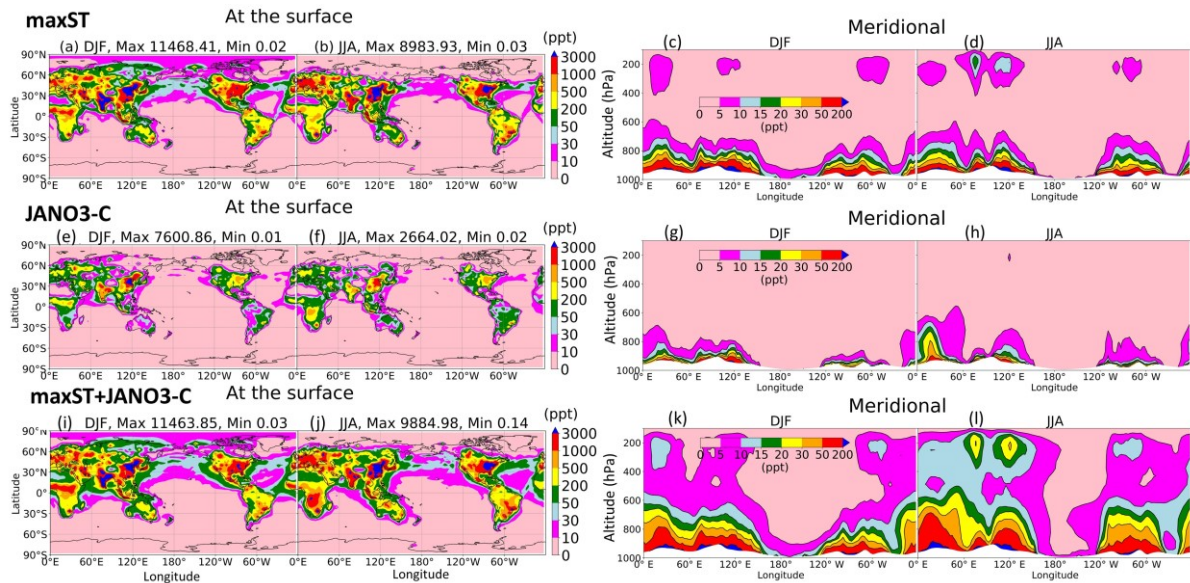


Figure S 12: HONO production in maxST (a-d), JANO3-C (e-h), and maxST+JANO3-C cases (i-l) at the surface layer (left panels) and meridional (right panels).

85

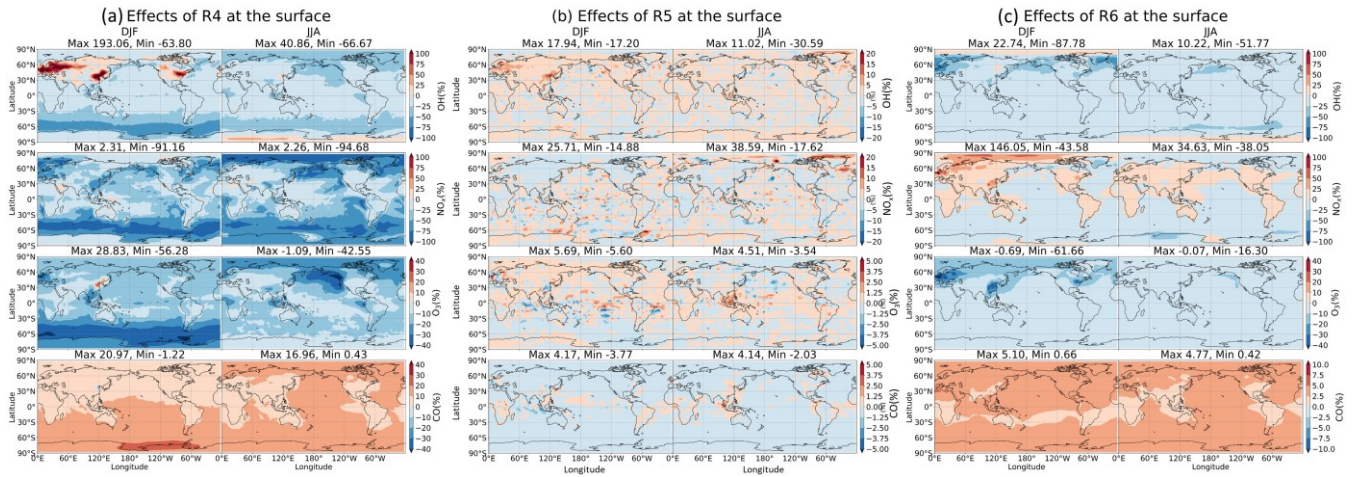


Figure S 13: Changes in the surface OH, NO_x, O₃, and CO concentrations by (R4), (R5), and (R6). The colorbar scale for each panel are different; (a) OH, NO_x (-100,100), O₃, CO (-40,40), (b) OH, NO_x (-20,20), O₃, CO (-5,5), (c) OH, NO_x (-100,100), O₃ (-40,40), CO (-10,10). Unit is %.

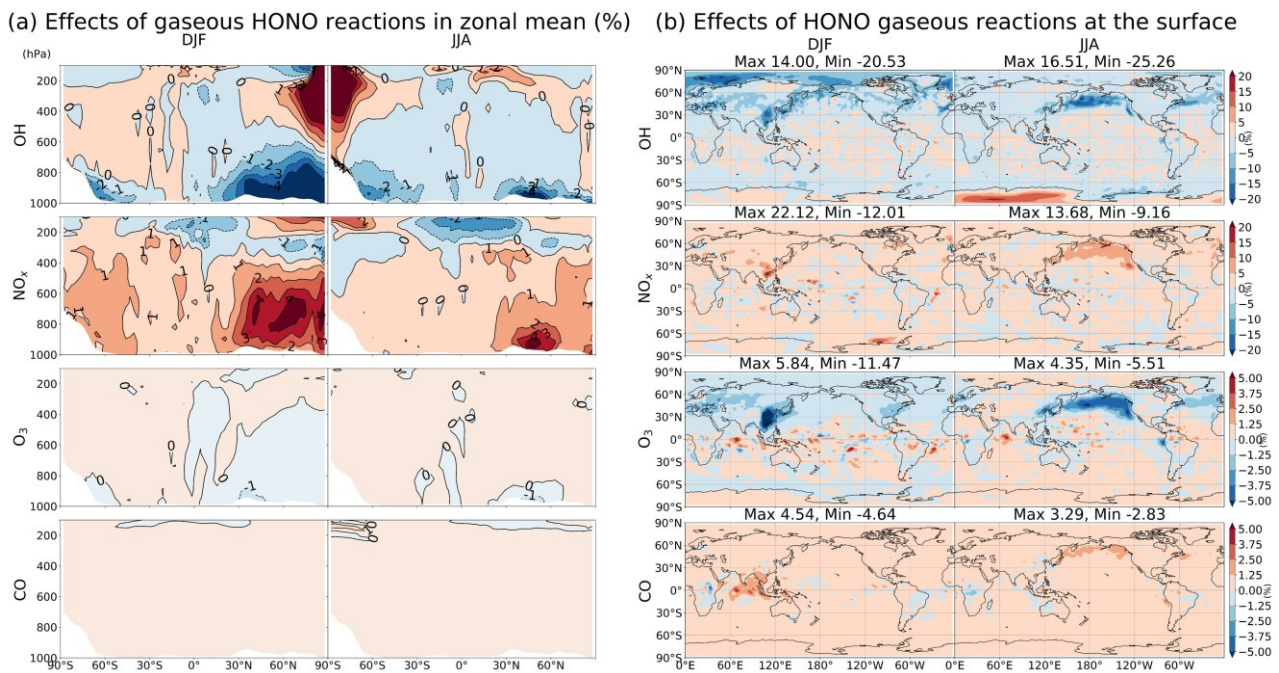


Figure S 14: Changes (%) in zonal mean (a) and at the surface (b) for OH, NO_x, O₃, and CO concentrations by gaseous HONO chemistry (R1, R2, R3). The colour scales for each panel are different.

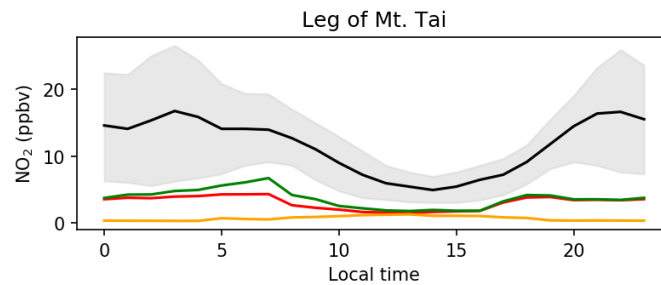


Figure S 15: NO₂ concentration at foot of Mt. Tai. At the foot, NO₂ levels in JANO3-A/B/C cases are overlaid by STD case. At the summit, simulated NO₂ levels are nearly zero in all cases (even in the OLD case) while Xue's averaged values were 1.5-3 ppb (minimum and maximum ranged from 0.2 – 5 ppb), thus not be illustrated.

95